Stacked graphene oxide and bio-sourced polyelectrolyte complexes thin coating for fire safe and sound absorbing flexible foams

Polymer Degradation and Stability 240 (2025) 111469

Contents lists available at ScienceDirect

Polymer Degradation and Stability

journal homepage: www.journals.elsevier.com/polymer-degradation-and-stability

Stacked graphene oxide and bio-sourced polyelectrolyte complexes thin coating for fire safe and sound absorbing flexible foams

Lorenza Maddalena [a], Louena Shtrepi [b], Massimo Marcioni [a], Alberto Fina [a], Federico Carosio [a,*]

[a] Dipartimento di Scienza Applicata a Tecnologia, Politecnico di Torino-Alessandria Campus, Viale Teresa Michel 5, 15121 Alessandria, Italy
[b] Dipartimento Energia "Galileo Ferraris", Politecnico di Torino, corso Duca degli Abruzzi 24, 10129 Torino, Italy

ARTICLE INFO

Keywords:
Polyelectrolyte complexes
Graphene oxide
Phytic acid
Gelatine
Foam
Flame retardancy
Sound absorption

ABSTRACT

Water based approaches aimed at the reduction of open cell foam flammability currently suffer from limited efficiency and practicability. In order to address this issue, this paper exploits the unique features of bio-sourced polyelectrolyte complexes (PECs) and high aspect ratio graphene oxide (GO), to deliver an efficient and high performing solution to foam flammability. To this aim, PECs encompassing gelatin and phytic acid were deposited on a brick-and-mortar graphene oxide polyacrylic acid (PAA) layer. This simple two-step deposition produces a stacked GO-PAA/PECs conformal coating on the 3D structure of the foam. The assembly produces a self-extinguishing behaviour during flammability tests in vertical configuration. The heat release rates are also reduced up to 50 % as assessed by forced combustion tests at 35 kW/m^2. This set of FR properties has never been achieved before with such low number of deposition steps. In addition, the sound absorbing properties of the coated foams were evaluated by impedance tube tests, highlighting how these foams could find application as fire-safe sound-absorbing panel. The proposed approach thus represents an efficient step forward in the design of multifunctional fire-safe foams with potential industrial scalability.

1. Introduction

Polyurethane foams (PU) are widely used in buildings and public transports as either cushioning materials or acoustic panels due to their low cost, versatility and performances [1]. In particular, the use of PU acoustic panels is common in several application fields such as offices, schools, theatres, cinemas, swimming pools, transportation etc. The foams are installed on the building walls, ceilings, roofs, floors and doors to address issues related to sound insulation and improve the acoustics (i.e. improve well-being and reduce the noise effects on health) [2]. However, the low density and the organic nature of PU pose a severe threat to safety as they can be easily ignited upon contact with a small flame or a cigarette. During combustion, the structural collapse of the foam and the production of incandescent droplets further increase the fire risk of this material that has been indeed identified as one of the main causes of a fire start and quick propagation [3]. To address this problem, flame retardant (FR) additives are conventionally employed in PU formulations in order to meet fire safety criteria. Halogenated flame retardants have been widely used for this purpose [4]. Unfortunately, due to environmental and health issues, the use of such halogenated compounds has been recently limited or prohibited in many application fields [4–8].

The research on halogen-free flame retardant solutions has therefore become a priority. Within this context, the development of FR solutions based on the concept of PU surface modifications has attracted great interest [9]. To this aim, the Layer by Layer (LbL) assembly has been widely employed as it is a water-based technique that operates under ambient conditions exploiting environmental benign substances. The LbL deposition is based on the subsequent adsorption of oppositely charged polyelectrolytes or nanoparticles on the substrate of choice, yielding either highly stratified or interpenetrating coatings, where electrostatic complexation occurs at molecular scale [10,11]. The LbL technique is extremely versatile as the parameters controlling the deposition (such as pH, temperature and ionic strength) can be finely tuned in order to allow for the assembly of a plethora of chemical species ranging from natural/synthetic polyelectrolytes to bio-macromolecules or nanoparticles [12]. In particular, LbL assemblies encompassing platelet-like nanoparticles, such as layered silicates [13–17] and

* Corresponding author.
E-mail address: federico.carosio@polito.it (F. Carosio).

https://doi.org/10.1016/j.polymdegradstab.2025.111469
Received 28 March 2025; Received in revised form 5 June 2025; Accepted 6 June 2025
Available online 7 June 2025

graphene related materials, [18,19] have been exploited for the preparation of FR PU characterized by low heat and smoke release during forced combustion tests. The highly efficient stratification of the employed nanoparticles as well as the formation of polyanion/polycation complexes at molecular scale have been suggested as the main reasons behind the success of these LbL coatings [20]. Conversely, intumescent-like formulations have been proven to require the support of a nanoparticle-based assembly in order to confer FR properties [21]. For example, chitosan/ammonium polyphosphate system has been reported to produce a self-extinguishing behaviour and reduced heat release rates only when deposited on top of a chitosan/vermiculite assembly [21]. However, despite the good results achieved, the relatively high number of deposition steps (i.e. 10–20) required to obtain sufficient FR performances currently limits the development of this FR approach [16]. The design of novel, high performing and easy to scale-up coating approaches is therefore both highly desirable and of applicative interest.

In this manuscript, we address this task by exploiting a two-step deposition procedure that combines the concept of the LbL assembly and the efficiency of water-soluble polyelectrolyte complexes (PECs). Soluble or colloidal stable PECs can be produced by direct mixing of two solutions containing oppositely charged polyelectrolytes under controlled conditions (concentration, pH, ionic strength), thus enabling the single-step deposition of coatings with LbL-like characteristics [22,23]. Due to this unique feature and the potential dramatic increase in deposition efficiency, PECs have rapidly attracted the interest of the scientific community becoming a widely investigated research field [24–28]. The use of PECs for the deposition of FR coatings has been first attempted on textiles yielding results similar to previously developed LbL assemblies [25,29]. Conversely, the development of FR PECs for PU foams has yet to match the performances of conventional LbL coatings. In order to address this performance gap, in this work, pre-formed PECs encompassing gelatin (Gel) and phytic acid (PhA) were stacked on top of a high aspect ratio graphite oxide nanoplatelets (GO)/polyacrylic acid (PAA) layer to produce an efficient FR coating for PU foams (Fig. 1).

GO and PAA were selected as first layer in order to provide mechanical support to the subsequent PECs layer. Gel and PhA have been chosen for the preparation of bio-based and environmentally friendly PECs with intumescent features. Such PECs composition aligns with the recent trend in the FR field that has witnessed a growing interest towards the use of biomass FR solutions for water-based coatings [25,30]. Indeed, Gel is a low-cost protein extracted from collagen, which may be recovered from wastes and by-products generated by industrial production based on animal origins [31]. Depending on pH, Gel can behave as either positive polyelectrolyte (below isoelectric point) or negative polyelectrolyte (above isoelectric point) [32–34]. PhA is a molecule contained in cereal grains, oil seeds and beans and consists in a six phosphateesters functionalized inositol with environmentally friendly, biocompatible, and nontoxic characteristics [35,36]. When compared to other biomass-derived FR chemicals, PhA represents the most interesting molecule given its relatively high phosphorus content (28 % wt) [37]. PhA can interact with positively charged polyelectrolytes, [38] and has been previously employed for the preparation of intumescent LbL coatings [39,40].

The formation of soluble Gel/PhA PECs and their adsorption on the anionic GO/PAA layer has been investigated by means of IR spectroscopy and SEM observations on model Si substrate. When transferred to PU foams, the stacked GO-PAA/Gel-PhA coating dramatically improved the FR properties by granting self-extinguishing behaviour during flammability tests in vertical configuration and reduced combustion rates during cone calorimetry, outperforming previously developed LbL assemblies. A practical application of these foams as fire safe acoustic panels is evaluated by impedance tube measurements.

2. Materials and methods

2.1. Materials

Open cell polyurethane foams of commercial grade with density 20 g dm^{-3} and 20 mm thick were bought from local warehouse, washed in ultrapure water and dried at 70 °C before use. Graphene oxide 1wt % dispersion (GO-X) was purchased from Avanzare Innovacion

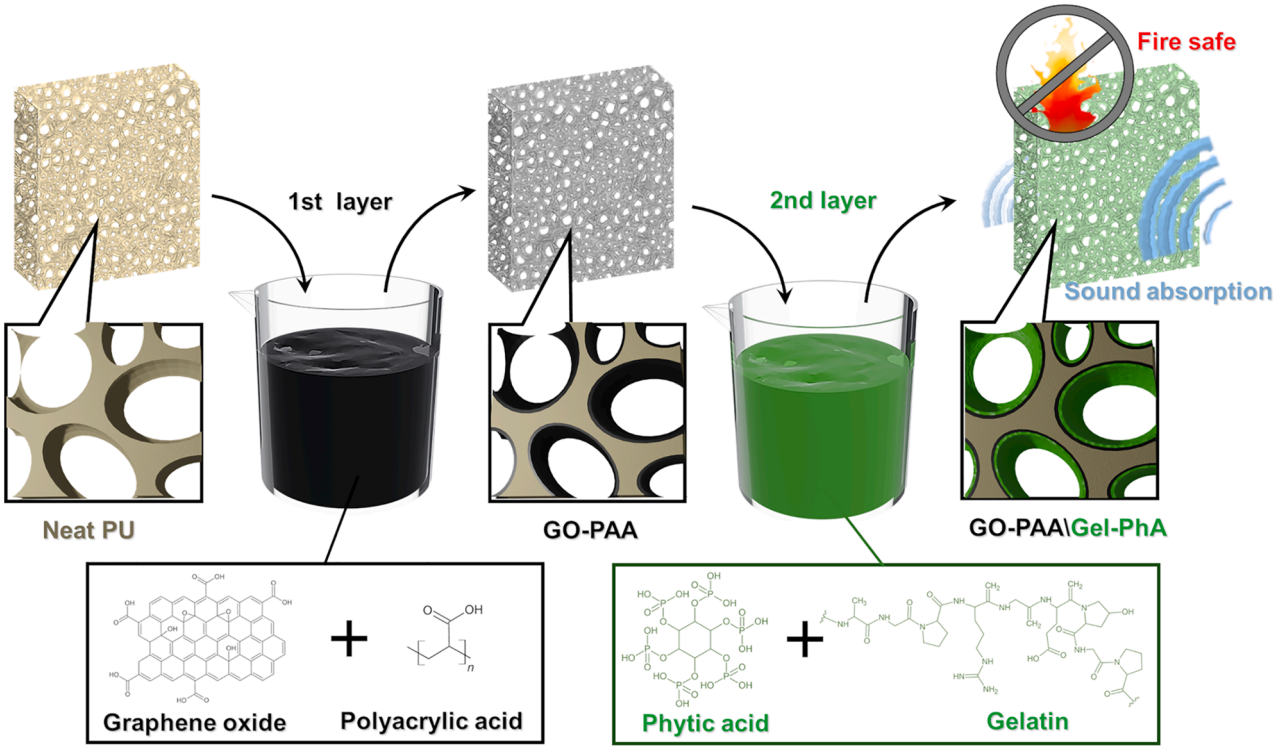

Fig. 1. Schematization of the deposition approach developed in this manuscript.

Tecnologica (Navarrete- La Rioja, Spain) and was used as received. Polyacrylic acid (PAA, average Mw 250,000, 35 wt % in water), gelatine (Gel, from cold water fish skin) and phytic acid (PhA, 50 wt % solution) were purchased from Merck (Milan, Italy). All solutions/dispersions were prepared with ultrapure water (resistivity 18.2 MΩ cm) supplied by Q20 Millipore system (Milan, Italy). A GO-PAA suspension was prepared by diluting 11.42 g of PAA with 1wt % GO dispersion to a final weight of 1000 g reaching a final PAA concentration of 0.4 wt %. Gel-PhA PECs solution was prepared by adding equal volumes (1:1 vol./vol.) of a 4 wt % phytic acid solution (pH 1.1, unmodified) to a 4 wt % gelatine solution (pH 6.5, unmodified) under magnetic stirring, achieving a final concentration of Gel-PhA equal to 2wt %−2wt %. Figure S1 collects digital images of the neat Gel and PhA solutions and snapshots acquired during their mixing for PECs preparation. Upon mixing PhA to Gel, temporarily insoluble PECs are formed as the solution immediately turns turbid with cloudy white filaments (Figure S1c) that eventually disappear leading to a homogeneous solution with pH 1.5 (Figure S1 d). At such pH, Gel behaves as a cationic polyelectrolyte with most of the amine groups protonated [34]. Conversely, the deprotonation of PhA is extremely limited as most of the phosphate groups are largely undissociated [41]. These conditions thus favour the formation of stable PECs where the protonated groups of Gel largely overcompensate the nearly undissociated phosphate groups of PhA therefore preventing the formation of insoluble PECs.

2.2. Coating deposition on model substrate

The coating was studied by FTIR in transmission mode on silicon wafer as a model substrate. BPEI (0.1 wt %) solution was used as primer in order to make the silicon surface prone to the GO-PAA adsorption. The silicon wafer was dipped 10 min in BPEI solution, rinsed with ultrapure water by 1 min dipping and then dried with compressed air. The negative layer of GO-PAA was deposited by dipping the silicon wafer 10 min and dried with compressed air and FTIR spectrum was recorded. The same procedure was repeated for the Gel-PhA PECs deposition.

2.3. Deposition procedure on PU foams

PU foams were dipped in the GO-PAA dispersion and then squeezed several times in order to allow the trapped air to escape while forcing the dispersion to completely fill the volume of the foam. The deposition time was set to 10 min. This condition is often employed in LbL assemblies in order to promote a homogeneous deposition of the coating constituents within the first layer pair [42]. After the deposition, the foams were removed from the dispersion and squeezed in order to remove the excess solution while targeting a wet pick-up of about 5 times the dry PU foam weight. Then, the wet foams were dried in a ventilated oven at 70 °C to constant weight. Once dried, the foams were then dipped in the Gel-PhA PECs solution following the procedure already described for the GO-PAA dispersion. Foams coated with this procedure are coded as GO-PAA/Gel-PhA. In order to provide complementary information on the effects of each deposition step, foams coated only by either the GO-PAA dispersion (coded GO-PAA) or the Gel-PhA PECs (coded Gel-PhA) were also prepared.

The coating add-on % was calculated as the dry weight gained after the treatment divided by the original weight of the foam (both uncoated and coated foam were dried in a ventilated oven at 70 °C to constant weight). The add-on % was found to be 10±1 %, 12±1 % and 40±2 % for GO-PAA, Gel-PhA and GO-PAA/Gel-PhA, respectively.

2.4. Characterization

The morphology of samples was investigated by scanning electron microscopy (SEM, Zeiss Evo 15, equipped with a ULTIM MAX 40 probe, Jena, Germany). The samples were positioned on conductive tape and gold sputtered prior to observation at beam voltage set to 3 kV. The coating assembly on model Si wafer was characterized by means of a FT-IR spectrometer (Perkin Elmer mod. Frontier, Waltham, MA, USA) in transmission mode (resolution 4 cm^{-1}, 16 scan). Flammability test were performed on 3 specimens for each coating formulation in horizontal configuration by the application of a 20 mm blue methane flame for 3 s on the short size of the specimen (50 × 150 × 20 mm^3) positioned on a metallic grid. During combustion, the formation of molten incandescent polymer drops was evaluated by placing dry cotton underneath the specimen. Vertical flammability test was performed on GO-PAA/Gel-PhA PU applying a blue methane flame on the short size of the foam clamped vertically for 3 s. The final residues were evaluated by weighting the specimens before and after the test. Prior to the tests, specimens were conditioned 23.0 ± 0.1 °C for 24 h at 50.0 %±0.1 R.H. in a climatic chamber. Forced combustion tests were performed on an oxygen consumption cone calorimeter (Noselab, Milan, Italy) using 100 × 100 × 20 mm^3 under 35 kWm^{-2} radiative flux. Measurements were performed 3 times for each formulation to obtain representative averages and experimental deviations. Time to Ignition (TTI), peak of Heat Release Rate and its average (pkHRR and avHRR, respectively), Total Heat Release (THR), Smoke Production Rate (SPR), Total smoke release (TSR) and final residue were evaluated. Average values are presented with their experimental deviations. The mechanical properties were evaluated by compression tests on a dynamometer (Instron 5966, 2 kN cell, Canton, MA, USA) by compressing 2 stacked samples of 200 × 200 × 18 mm^3 between two horizontal plates and following the EN ISO 2439 standard (60 % compression, deformation speed 100 mm/min). An additional set of GO-PAA/Gel-PhA coated samples (80 × 60 × 18 mm^3) was also compressed (60 % compression, deformation speed 10 mm/min) and then tested by vertical flammability tests. Prior to the tests, samples were conditioned 23.0 ± 0.1 °C for 48 h at 50.0 %±0.1 R.H. in a climatic chamber.

Acoustic measurements have been performed in an impedance tube in accordance with ISO 10,534–2 (two-microphone technique) in order to measure the normal-incidence absorption coefficient (α_0). The advantages of this method rely on the possibility to obtain measurements using small specimens suitable to the aim of this investigation. These measurements were conducted by means of an impedance tube HW-ACT-TUBE (Siemens, Munich, Germany), which has a diameter of 35 mm and is equipped with two ¼ inch flush mounted GRAS 46BD (GRAS, Holte, Denmark). The method allows to have accurate sound pressure amplitude and phase measurements in the whole frequency range of interest, i.e. 100–5000 Hz. The measurements have been performed on 10 specimens for each formulation evaluated. The specimens were cut from uncoated and coated foam panels (thickness 20 mm) with a circular cutter with a diameter of 35 mm.

3. Results and discussion

3.1. Coating assembly on model substrate and PU foam

The occurrence of electrostatic interactions between the anionic GO-PAA dispersion and the cationic Gel-PhA solutions was preliminary investigated by directly mixing the two components (Figure S2). The formation of non-soluble complexes from a given set of polyelectrolytes/nanoparticles is considered a preliminary condition for their exploitation in a LbL assembly. Upon adding the Gel-PhA solution to the GO-PAA dispersion, complexes are produced leading to the formation of macroscopic aggregates (Figure S2), thus suggesting the interactions between GO-PAA and Gel-PhA may be sufficiently strong to drive a LbL assembly. The coating assembly was then investigated by FTIR in transmission mode on silicon wafer as model substrate, after BPEI was deposited as a primer layer. Fig. 2 collects a schematization of the adopted procedure, the acquired FTIR spectra and the SEM micrograph of the coating cross section. Figure S3 collets the spectra of the neat components deposited by drop-casting on Si Wafer.

The adsorption of the anionic GO-PAA layer yields a spectrum

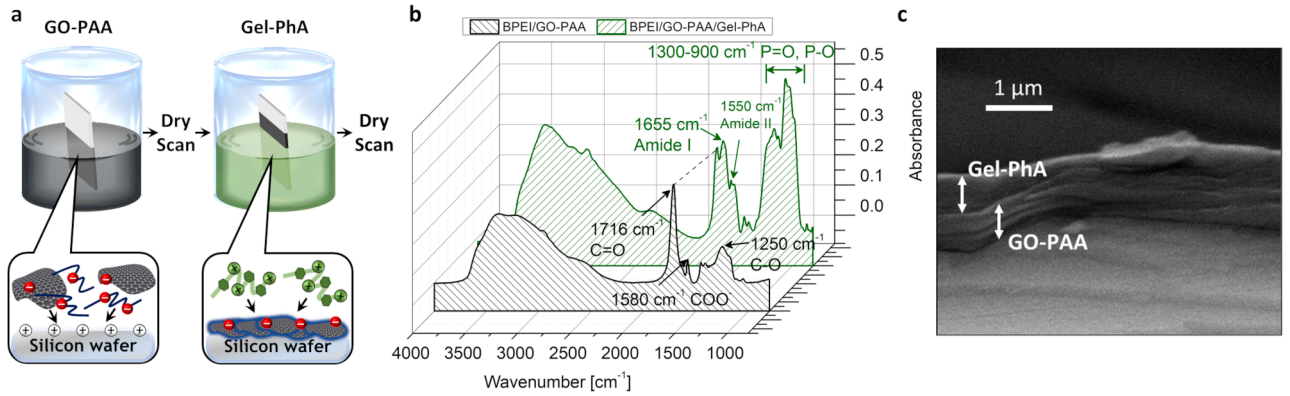

Fig. 2. Coating assembly on model Si substrate: (a) schematization of the coating procedure, (b) FTIR spectra of the GO-PAA and GO-PAA/Gel-PhA assembly and (c) high magnification SEM micrograph of the cross-section of the assembled GO-PAA/Gel-PhA.

characterized by the signals of both components. The most intense peaks are linked to the COOH functional groups of both GO and PAA. $C = O$ stretching is clearly observable at 1716 cm^{-1}, the carboxylate signal is found at 1580 cm^{-1} whereas a less intense signal occurring at 1250 cm^{-1} is attributed to the C—O stretching coupled with O—H in-plane bending [43]. A broad band in the 3500–2500 cm^{-1} region is due to the O—H stretching of hydroxyl groups and adsorbed water. The broadness of this latter band reflects the hydrogen bonding between OH groups, which is well documented for PAA [43]. The subsequent adsorption of the Gel-PhA PECs layer significantly modifies the spectrum yielding new signals related to both Gel and PhA functional groups. In particular, Gel characteristic amide I and II peaks are found at 1655 and 1550 cm^{-1}, respectively [44]. Meanwhile, a new set of signals (1300–900 cm^{-1}) appears in the finger print region and is ascribed to the PhA phosphate ester groups, including $P = O$ stretching and P-O deformation modes [45,46]. The coating cross section was also investigated by SEM (Fig. 2c). The collected micrographs highlight the deposition of a homogeneous and dense coating (ca. 1 µm thick) where the Gel-PhA PECs and the GO-PAA layers are clearly observable. These results confirm the occurrence of bi-layer stacked structure displaying Gel-PhA PECs supported by a GO-PAA layer where the GO platelets are oriented parallel to the surface. The deposition of GO-PAA/Gel-PhA assembly was then applied to open cell PU foams. Samples coated by either GO-PAA or Gel-PhA were also prepared as references. The coating morphology on PU foams was investigated by means of SEM (Fig. 3).

Neat PU exhibits the typical 3-dimensional (3D) structure of open cell foams characterized by a uniform and smooth surface. The GO-PAA deposition considerably modify this morphology by producing a rough and homogenous coating that wraps the 3D structure of the PU foam. The presence of GO nanoplates embedded within PAA is clearly visible in high magnification micrographs (Fig. 3b), causing an increase in surface roughness. The deposition of the Gel-PhA PECs alone does not produce a continuous coating but leads to the formation of PECs aggregates that appear to be randomly distributed on the PU walls (as pointed out by EDS analyses in Figure S4). Conversely, when the Gel-PhA PECs are stacked on the GO-PAA layer, a homogeneous and smooth coating is achieved (Fig. 3d). This result is ascribed to the presence of the previously adsorbed GO-PAA layer that, thanks to the formation of hydrogen bonds between undissociated COOH groups of PAA/GO and PU[47], acts as a functional activation layer for deposition of Gel-PhA PECs.

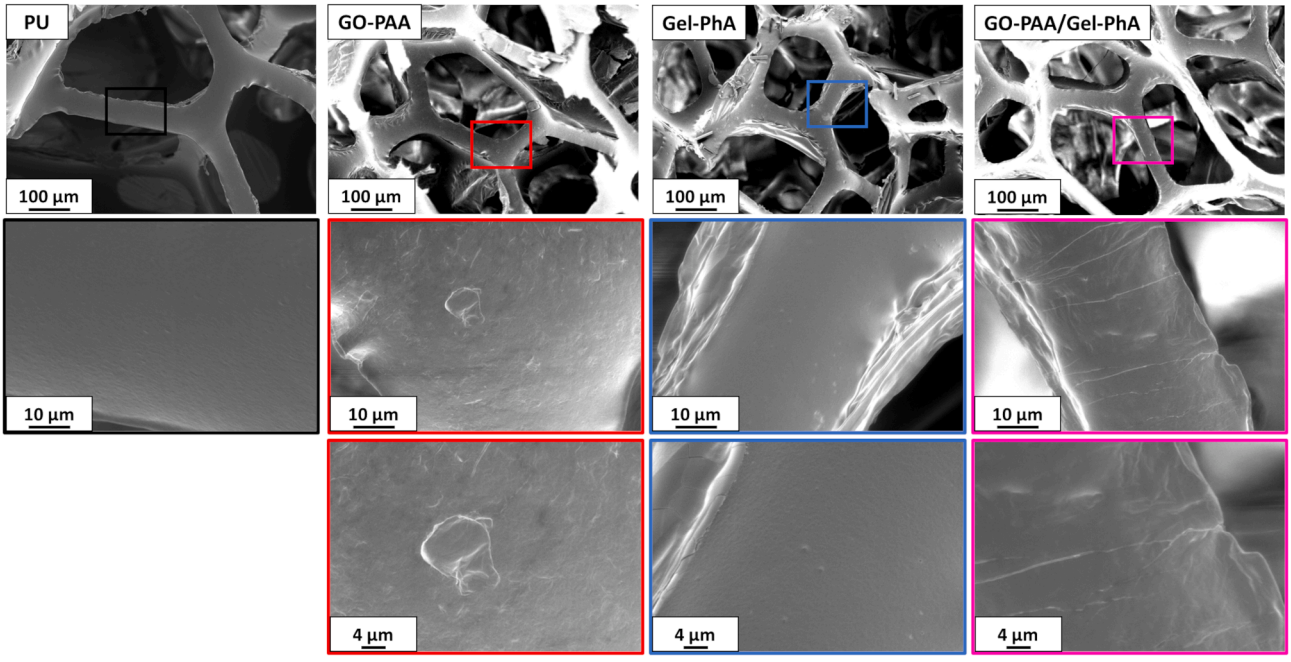

Fig. 3. SEM micrographs of untreated and treated PU.

3.2. Flame retardancy of coated PU foams

The flame retardancy performance was assessed by evaluating the coated foam reaction to the exposure to a small flame (flammability test) or an impinging heat flux typical of developing fires (forced combustion test in cone calorimeter) [48]. This approach provides a complete set of information on the coated foam propensity to initiate or spread a fire [49]. The uncoated and coated foams behaviour during flammability tests are reported in Fig. 4, while Fig. 5 collects cone calorimetry plots. Table S1 and Table S2 summarize flammability and forced combustion data, respectively.

Horizontal flammability was first evaluated as this represent common testing condition for foamed materials in many application fields [50]. Upon flame application the neat PU immediately ignites and burns vigorously, releasing incandescent molten droplets that are able to ignite the dry cotton positioned underneath the foam. This latter setup represents a common practice of flammability standards (e.g., UL 94 standard) aimed at evaluating the ability of the tested materials to propagate the flame to other ignitable materials. This behaviour is particularly dangerous as it can lead to a detrimental increase in fire spreading rates in real fire scenarios [51]. The flame almost completely consumes the PU leaving a brittle and thin residue, at the end of the test, in the range of 8 % of the initial specimen mass.

The deposition of the GO-PAA layer considerably reduces the flame spread rate (from 4.9 to 1.8 mm/s for neat PU and GO-PAA treated PU, respectively) while suppressing the melt-dripping and largely preserving the structure of the foam. Although the flame spread is not blocked, only the outer portion of the foam is actually damaged as demonstrated by the high final residue (70 % wt) and visual observation of the foam cross-sections (Figure S5). Conversely, the presence of the Gel-PhA layer alone barely suppressed melt-dripping but did not preserve the structure of the foam that collapsed in a thin and brittle residue accounting for 27 % of the starting weight. Interestingly, the stacked GO-PAA/Gel-PhA assembly showed a behaviour where no flame persists on the specimen after the removal of the methane flame (Fig. 4a). Such impressive result points out the great FR efficiency of the stacked configuration that leaves the coated foam almost undamaged at the end of the test (final residue > 99 %wt). The observed behaviour is in agreement with previously developed conventional LbL coatings encompassing intumescing formulations deposited on top of clay rich layers [21].

Since the GO-PAA/Gel-PhA treated foams displayed an optimal FR behaviour during flammability tests in horizontal configuration, the vertical setup was also investigated. This latter represents a more severe testing condition, required for the evaluation the fire safety of dense materials for many practical applications (e.g. transportation, buildings, etc.) [52]. In this configuration, the neat PU is immediately ignited with flames reaching the top of the specimen. During combustion, a conspicuous melt-dripping takes place and eventually leads to the complete detachment of the burning foam from the clamp. Conversely, the GO-PAA/Gel-PhA foams display a self-extinguishing behaviour, while showing no melt-dripping. At the end of the test, the foam appears almost undamaged with minimal weight loss (i.e., ≤2 %), thus highlighting optimal FR performances. Notably, these properties are maintained even after being compressed to 60 % deformation thus suggesting a good adhesion and flexibility of the deposited GO-PAA/Gel-PhA coating (Figure S6). Indeed, while the coated foams are stiffer than the uncoated ones, the ability to recover the deformation after a compressive loading/unloading cycle is maintained. Cone calorimetry tests were performed to investigate the combustion behaviour of neat and untreated foams (Fig. 5). Figure S7 collects the images of the residues collected at the end of the test.

When exposed to the heat flux in forced combustion test, the neat PU

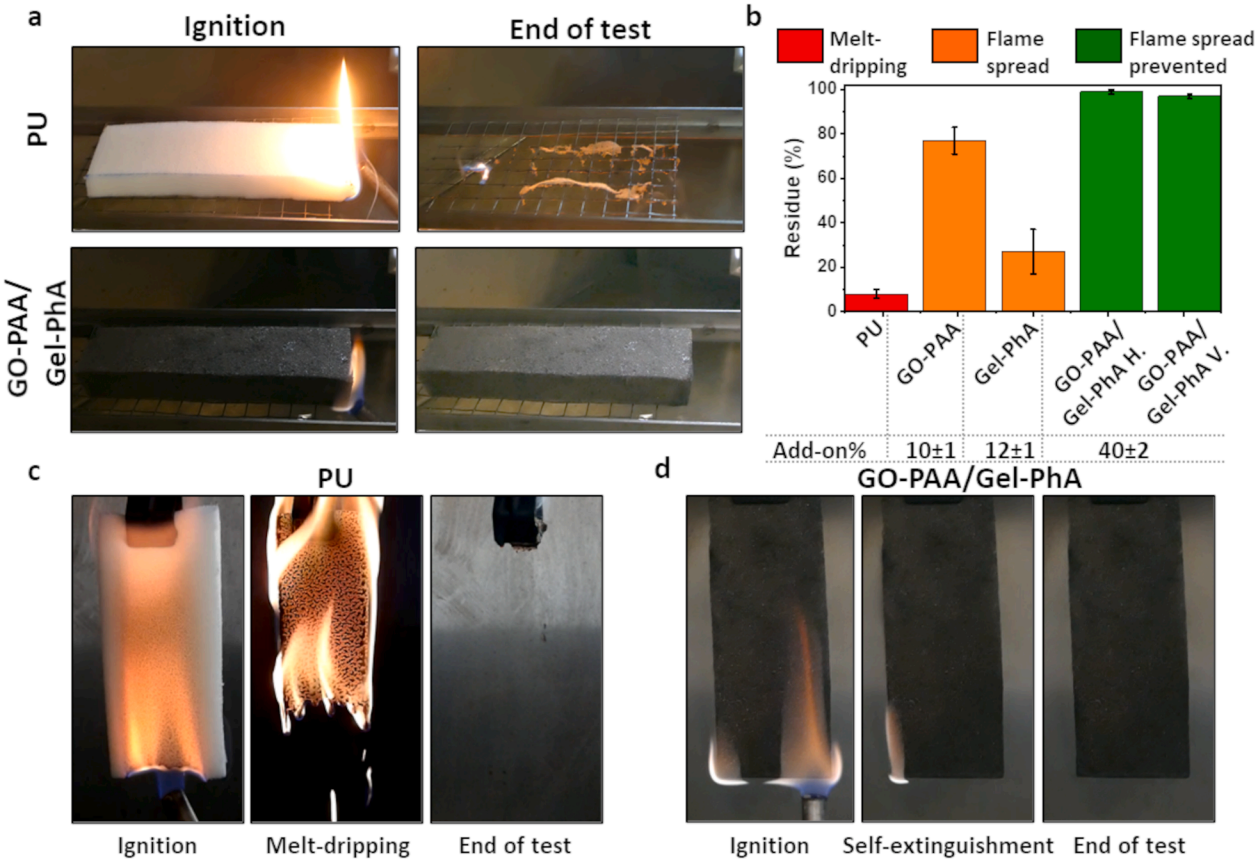

Fig. 4. Flammability test of untreated and GO-PAA/Gel-PhA treated PU: a) snapshots during horizontal test, b) average residues after flammability tests in horizontal (H) and vertical (V) configuration, c) and d) snapshots during vertical test.

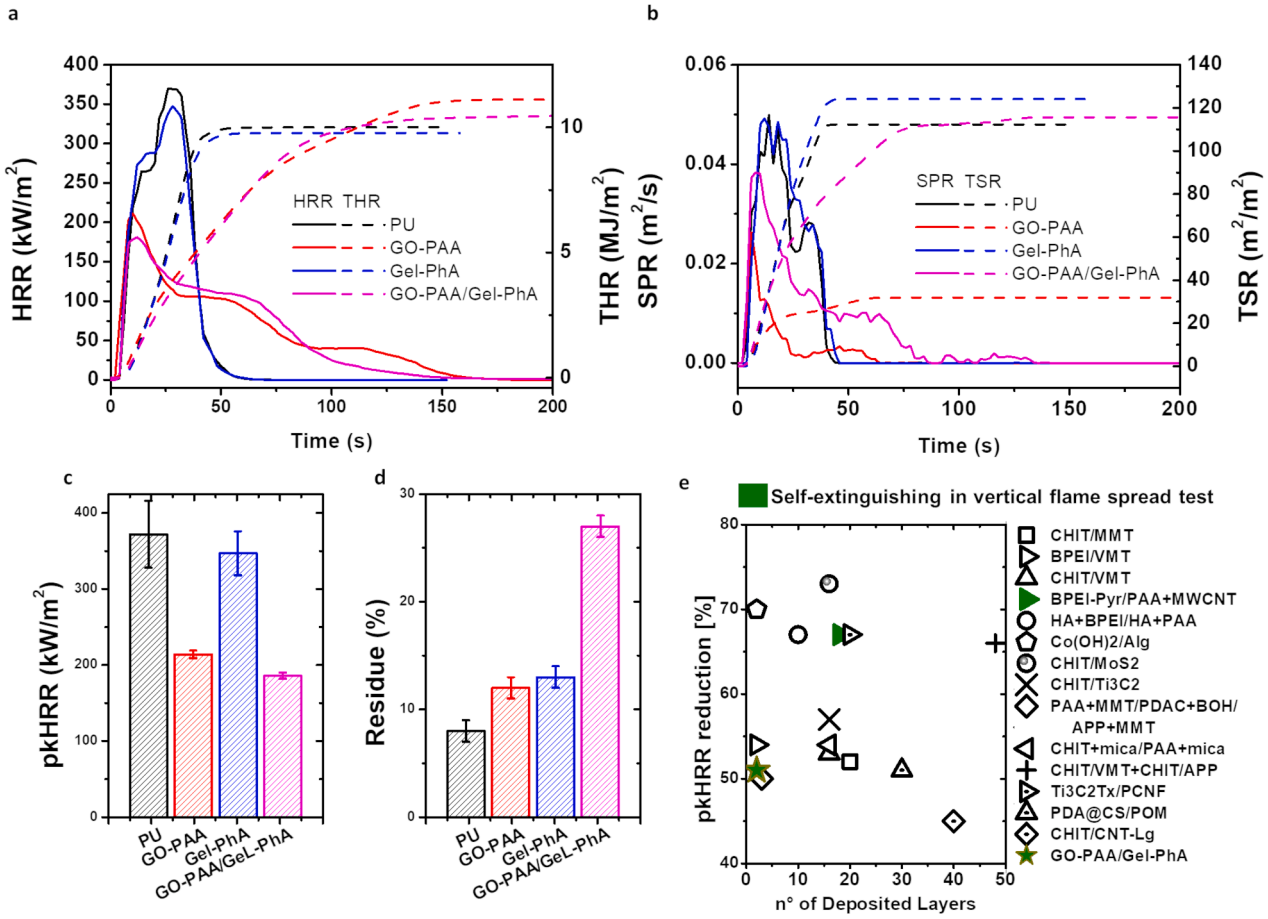

Fig. 5. Cone calorimetry test results: a) HRR and THR vs time plots, b) SPR and TSR vs time plots, c) pkHRR values, d) residue % and e) comparison with literature background comprising LbL and PECs coating on open cell PU foams.

quickly ignites while its 3D structure rapidly collapses producing a pool of low viscosity liquid with a sudden increase in combustion rate (pkHRR is 371 ± 44 kW/m^2). The foam is completely consumed leaving almost no residue at the end of the test (Figure S7). In strong contrast with neat PU, the presence of the GO-PAA layer is capable of limiting the foam collapsing thus modifying the PU burning behaviour and eventually reducing the pkHRR to 214 ± 5 kW/m^2 (- 42 %). The HRR plot broadens (Fig. 5a), which is typical when high aspect ratio nanoparticles are included within the coating [20]. Smoke parameters are also affected with reduced SPR values and a substantial decrease in TSR from 112 ± 7 to 32 ± 9 m^2/m^2 (- 72 %) (Fig. 5b). The Gel-PhA PECs do not produce beneficial effects when deposited as a stand-alone layer. Indeed, the pkHRR (347 ± 29 kW/m^2) remains within the experimental error, whereas TSR is increased to160 m^2/m^2. Conversely, the stacked configuration GO-PAA/Gel-PhA displays the same burning behaviour of GO-PAA PU with improved reductions in combustion rates (pkHRR is 186 ± 4 kW/m^2, i.e. −50 % in with respect to neat PU). THR values remain within the experimental error measured for neat PU. This suggests that the PU is almost completely consumed and the presence of the coating mainly affects the volatile release rate thus producing reduced HRR values. Despite the unaffected THR values, the ability to preserve the structure of the foam (Figure S7) coupled with greatly reduced HRR would improve the fire safety of the coated foams as the structural collapsing and the high HRR of PU foams have been often correlated with a propensity to increase fire spread rates in a real fire scenario [51]. Smoke parameters remained equivalent to PU, within the experimental uncertainty. The obtained FR results evidence how the GO-PAA/Gel-PhA coating delivers a noticeable FR performance when applied to PU foams. Indeed, the coated foams achieve rapid self-extinguishment in both horizontal and vertical configurations as well as combustion rates below 200 kW/m^2.

The stacked bilayer coating developed in this work was further benchmarked with other coating formulations deposited in a LbL fashion on PU foams (Fig. 5e) [15,21,53–64]. As reported in Fig. 5e, most of the coating formulations developed in the literature can achieve pkHRR reductions in the 40–70 % range. However, very few systems are reported to grant a self-extinguishing behaviour in vertical configuration and such performance is linked to large deposition cycles (e.g. 18 deposition steps). In strong contrast, to the best of the authors' knowledge, the coating developed in the present study is currently the only one capable of achieving a substantial reduction in pkHRR and a self-extinguishing behaviour in vertical configuration with only 2 deposition steps. The stacked GO-PAA/Gel-PhA assembly thus represent the optimal balance between FR properties and processing conditions.

3.3. Post combustion residue analysis

During combustion, the presence of either the GO-PAA or GO-PAA/Gel-PhA coating preserved the macroscopic structure of the foams as demonstrated by digital images of the residues collected after cone calorimetry tests (Figure S7). In order to further analyse these residues, their microscopic structure has been imaged by SEM (Fig. 6 and Figure S8). The GO-PAA PU displays the formation of a charred residue resembling the original 3D structure of the foam. Struts and joints are replaced by thin and compact shell made of GO nanoplatelets held together by a continuous charred matrix produced during PAA and PU thermal decomposition. The presence of multiple cracks and partially collapsed sections suggests that the produced structure is extremely

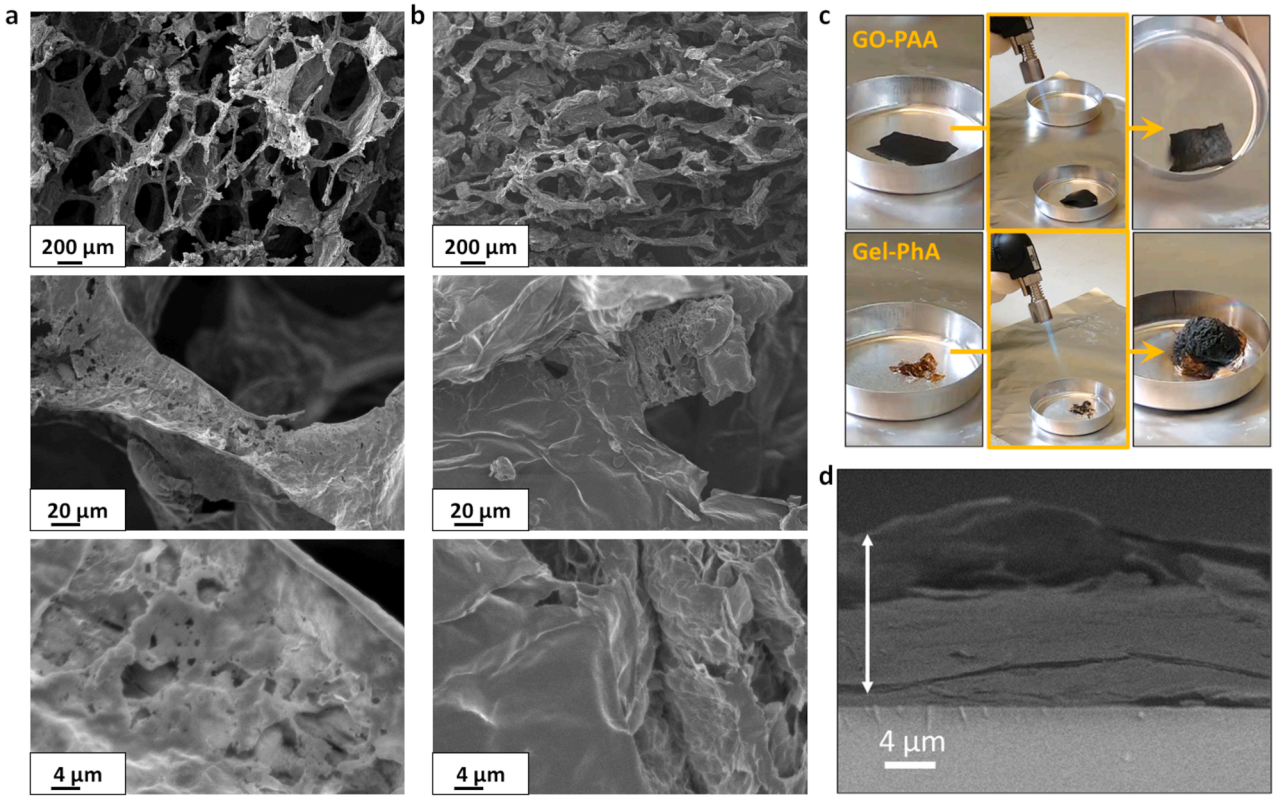

Fig. 6. Post combustion residue SEM investigation of GO-PAA (a) and GO-PAA/Gel-PhA (b) coated foams after cone calorimetry tests. Digital images of GO-PAA and Gel-PhA PECs dried films when exposed to a flame (c) and SEM micrograph of GO-PAA/Gel-PhA on model Si wafer after 35 kW/m^2 heat flux exposure (d).

brittle. The GO-PAA/Gel-PhA PU also preserves its original open cell structure by producing a porous and expanded shell having dimensions greater than the one produced by GO-PAA. EDS analyses and maps pointed out the presence of C, P and O as the main elements constituting the expanded structures (Figure S9). This suggests a somewhat intumescent feature of the Gel-PhA PECs, that, thanks to the GO-PAA supporting layer, can fully develop an expanded protective barrier during combustion.

Indeed, as reported in Fig. 6c, the application of a direct flame to a dried PECs film results in the formation of a carbon-based expanded structure due to the release of carbon dioxide and ammonia from gelatine decomposition catalysed by the presence of phytic acid [65]. A similar behaviour is also observed for the stacked GO-PAA/Gel-PhA deposited on model Si wafer that, after being exposed to the cone calorimetry heat flux, produced an expanded structure averagely 10 times thicker than the original coating. It is worth mentioning that the Gel-PhA PECs alone cannot achieve the same intumescent effect when deposited as a stand-alone layer on PU where a collapsed structure with no substantial FR effects is instead produced during combustion (Figure S7). Based on the collected FR results and post combustion residue investigation, it is possible to preliminary discuss a general FR mechanism for the GO-PAA/Gel-PhA coated foams. Upon exposure to a flame or a heat flux, the GO-PAA layer prevents the foam structural collapsing and provides support to the intumescence process of the Gel-PhA PECs. This latter develops an expanded carbonaceous structure that, in combination with the layered structure of the underlying GO-PAA, limits heat and mass transfer from and to the flame. In turns, this reduces the heat flux from the flame, allowing to reach self-extinguishment in flammability test and a significant reduction of the combustion rate in forced combustion test. In addition, it is worth considering that, while it appears that the main FR mechanism is exerted in the condensed phase, a gas phase action related to PhA might also be possible. Indeed, PhA has been shown to act as a flame inhibitor and exert a gas phase FR action when employed in FR coatings deposited on PU [37,66].

3.4. Acoustic properties

The effects of the GO-PAA/Gel-PhA coating on the foam sound absorbing properties have been preliminary investigated aiming at practical application as fire safe acoustic panels. Uncoated and coated foams were tested in the 100–5000 Hz frequency range, which is where most everyday sounds fall and is therefore widely employed for evaluating insulating materials for building applications [67]. The typical mechanisms for flexible PU sound absorption is linked to the vibration of the material that physically disperse the gas molecules in air, thus generating frictional forces that dissipate sound energy [68]. Fig. 7 reports the digital images of the employed impedance tube apparatus and the normal-incidence sound absorption coefficient (α_0) vs frequency for the uncoated and GO-PAA/Gel-PhA coated foams.

The results of the acoustic test showed some differences between the uncoated and coated PU foams. Indeed, as reported in Fig. 7, the unmodified foam reaches a sound absorption of 0.9 at about 3500 Hz while it can be observed that the sound absorption properties improve at lower frequencies up to 3000 Hz after the deposition of the GO-PAA/Gel-PhA coating. Above this frequency, the performance of the GO-PAA/Gel-PhA foam is slightly lower than the untreated PU. As reported in literature, [69] such effect is usually observed when the deposition of a coating increases the amount of the foam closed pores eventually producing a tortuous and longer path for the acoustic waves. This phenomenon was not observed for the GO-PAA/Gel-PhA foam (Fig. 3). The observed behaviour can be instead related to the increase in density of the coated foam (from ≈ 20 kg/m^3 to ≈ 28 kg/m^3) that has been reported to produce a similar impact in the absorption efficiency vs frequency plots [70]. In addition, the increase in stiffness of the coated foams (Figure S6) and the decrease in the foam mean pore size might also lead to an

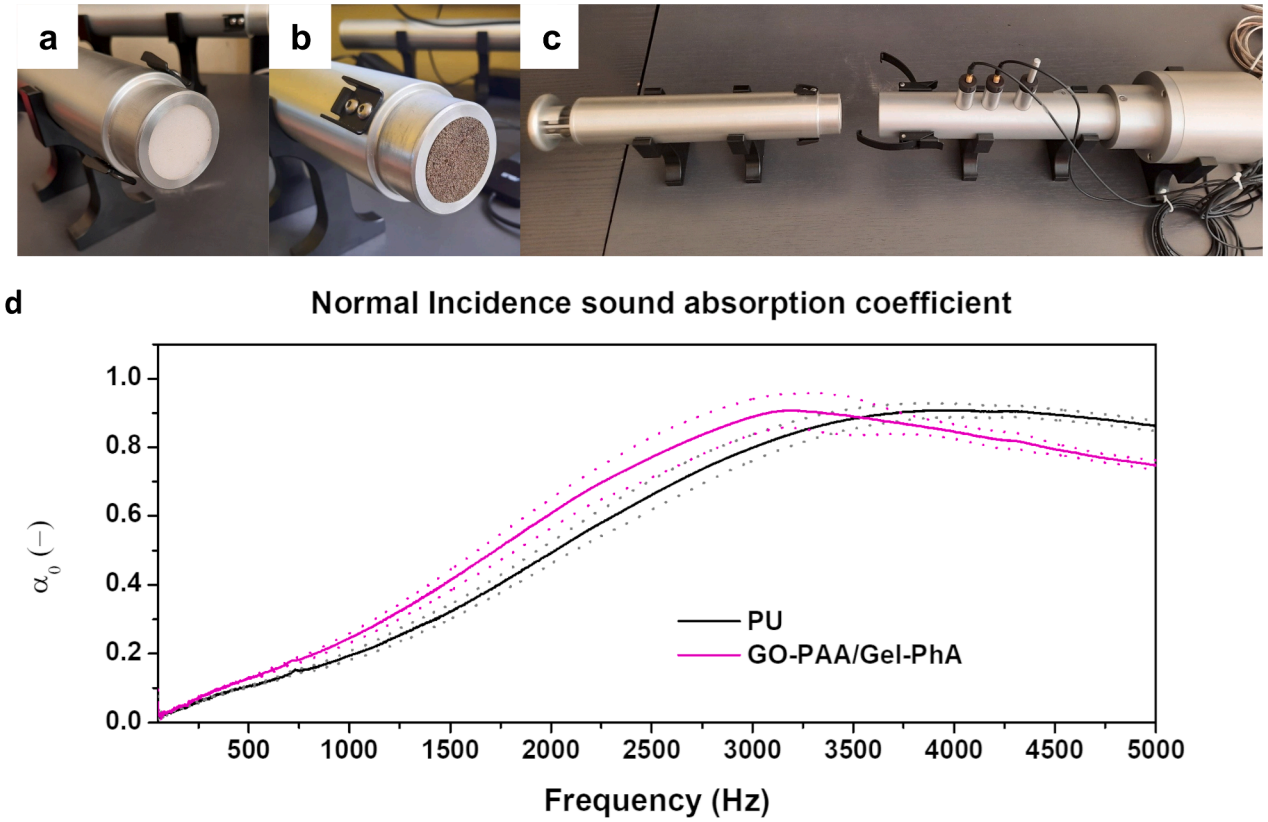

Fig. 7. Specimen inserted in the impedance tube and set-up of the HW-ACT-TUBE (a-c). Measured normal-incidence sound absorption coefficient and standard deviation for PU and GO-PAA/Gel-PhA (d).

increase in the airflow resistivity and therefore in the sound absorption performance [71].

4. Conclusions

A novel flame retardant coating solution to reduce the fire threat of PU foams has been developed by exploiting bio-sourced PECs and high aspect ratio graphene oxide. To this aim, PECs with intumescent-like behavior encompassing gelatin and phytic acid have been deposited on top of a brick-and-mortar graphene oxide polyacrylic acid layer by an easy and efficient two-steps deposition approach. When applied on PU foams, the procedure yields a homogeneous and continuous coating that conformally adapts to the complex 3D structure of the foam. The GO-PAA/Gel-PhA coated foams are capable of self-extinguishing the flame and considerably reduce combustion rates (−50 % in pkHRR) during flammability in vertical configuration and cone calorimetry tests, respectively. A comparison with the literature background further pointed out the efficiency of the proposed coating design that delivers a unique set of FR properties with only 2 deposition steps. A possible FR mechanism was also proposed based on the performed FR characterization and post-combustion residue investigation. The GO-PAA layer has been found crucial in preventing the foam structural collapsing and in providing mechanical support to the formation of an expanded protective structure from the Gel-PhA PECs. The so-formed barrier hinders the release of flammable volatiles feeding the flame eventually producing the observed excellent FR performances. The effects of the coating on the foam acoustic properties have been investigated by impedance tube tests. The presence of the coating improves the sound absorption properties at low frequencies up to 3000 Hz thus suggesting a possible application of the coated foams as fire safe and sound absorbing panel. Future works might be focused on in-depth investigations of airflow resistivity as well as porosity and tortuosity measurements in order to correlate the coating morphology to the observed acoustic behavior. In conclusion, by exploiting the versatility of a LbL-derived assembly and the efficiency of PECs, this paper presented a novel strategy for the design of functional coatings with tailorable FR actions. The proposed approach opens up to the development of efficient, high performing and industrially viable coating solutions, that could be possibly applied to other porous materials.

CRediT authorship contribution statement

Lorenza Maddalena: Writing – original draft, Investigation. **Louena Shtrepi:** Writing – original draft, Investigation. **Massimo Marcioni:** Visualization. **Alberto Fina:** Writing – review & editing, Funding acquisition. **Federico Carosio:** Writing – review & editing, Visualization, Supervision, Conceptualization.

Declaration of competing interest

The authors declare that they have no known competing financial interests or personal relationships that could have appeared to influence the work reported in this paper.

Acknowledgements

Financed by the European Union - NextGenerationEU (National Sustainable Mobility Center CN00000023, Italian Ministry of University and Research Decree n. 1033 - 17/06/2022, Spoke 11 - Innovative Materials & Lightweighting). The opinions expressed are those of the authors only and should not be considered as representative of the European Union or the European Commission's official position. Neither the European Union nor the European Commission can be held responsible for them.

Supplementary materials

Supplementary material associated with this article can be found, in the online version, at doi:10.1016/j.polymdegradstab.2025.111469.

Data availability

Data will be made available on request.

References

[1] N.V. Gama, A. Ferreira, A. Barros-Timmons, Polyurethane foams: past, present, and future, Materials 11 (10) (2018) 1841.
[2] Y. Tao, M. Ren, H. Zhang, T. Peijs, Recent progress in acoustic materials and noise control strategies – a review, Appl. Mater. Today 24 (2021) 101141.
[3] A.B. Morgan, Revisiting flexible polyurethane foam flammability in furniture and bedding in the United States, Fire Mater. 45 (1) (2021) 68–80.
[4] S. Bocchini, G. Camino, Halogen-containing flame retardants, Fire retard. Polym. Mater. 2 (2010).
[5] A.B. Morgan, The future of flame retardant polymers – unmet needs and likely new approaches, Polym. Rev. 59 (1) (2019) 25–54.
[6] J. Sun, Q. Chen, Y. Han, H. Zhou, A. Zhang, Emissions of selected brominated flame retardants from consumer materials: the effects of content, temperature, and timescale, Environ. Sci. Pollut. Res. 25 (24) (2018) 24201–24209.
[7] K. English, Y. Chen, L.-M Toms, P. Jagals, R.S. Ware, J.F. Mueller, et al., Polybrominated diphenyl ether flame retardant concentrations in faeces from young children in Queensland, Australia and associations with environmental and behavioural factors, Env. Res 158 (2017) 669–676.
[8] G. Stieger, M. Scheringer, C.A. Ng, K. Hungerbühler, Assessing the persistence, bioaccumulation potential and toxicity of brominated flame retardants: data availability and quality for 36 alternative brominated flame retardants, Chemosphere 116 (2014) 118–123.
[9] G. Malucelli, F. Carosio, J. Alongi, A. Fina, A. Frache, G. Camino, Materials engineering for surface-confined flame retardancy, Mater. Sci. Eng.: R: Rep. 84 (2014) 1–20.
[10] G. Decher, Fuzzy nanoassemblies: toward layered polymeric multicomposites, Science 277 (5330) (1997) 1232–1237.
[11] Park SY, M.F. Rubner, A.M. Mayes, Free energy model for layer-by-layer processing of polyelectrolyte multilayer films, Langmuir 18 (24) (2002) 9600–9604.
[12] G. Decher, J.D. Hong, J. Schmitt, Buildup of ultrathin multilayer films by a self-assembly process: III. Consecutively alternating adsorption of anionic and cationic polyelectrolytes on charged surfaces, Thin Solid Films 210-211 (1992) 831–835.
[13] Y.-C. Li, Y.S. Kim, J. Shields, R. Davis, Controlling polyurethane foam flammability and mechanical behaviour by tailoring the composition of clay-based multilayer nanocoatings, J. Mater. Chem. A 1 (41) (2013) 12987–12997.
[14] P. Chen, Y. Zhao, W. Wang, T. Zhang, S. Song, Correlation of Montmorillonite sheet thickness and flame retardant behavior of a Chitosan–Montmorillonite nanosheet membrane assembled on flexible polyurethane foam, Polymers 11 (2) (2019) 213.
[15] S. Lazar, F. Carosio, A.-L. Davesne, M. Jimenez, S. Bourbigot, J. Grunlan, Extreme heat shielding of clay/Chitosan Nanobrick wall on flexible foam, Acs. Appl. Mater. Inter. 10 (37) (2018) 31686–31696.
[16] A.A. Cain, C.R. Nolen, Y.-C. Li, R. Davis, J.C Grunlan, Phosphorous-filled nanobrick wall multilayer thin film eliminates polyurethane melt dripping and reduces heat release associated with fire, Polym. Degrad. Stabil. 98 (12) (2013) 2645–2652.
[17] H.-B. Chen, D.A. Schiraldi, Flammability of polymer/clay aerogel composites: an overview, Polym. Rev. 59 (1) (2019) 1–24.
[18] F. Carosio, L. Maddalena, J. Gomez, G. Saracco, A. Fina, Graphene oxide exoskeleton to produce self-extinguishing, nonignitable, and flame resistant flexible foams: a mechanically tough alternative to inorganic aerogels, Adv Mater Interfaces 5 (23) (2018) 1801288.
[19] L. Maddalena, F. Carosio, J. Gomez, G. Saracco, A. Fina, Layer-by-layer assembly of efficient flame retardant coatings based on high aspect ratio graphene oxide and chitosan capable of preventing ignition of PU foam, Polym. Degrad. Stabil. 152 (2018) 1–9.
[20] L. Maddalena, J. Gomez, A. Fina, F. Carosio, Effects of graphite oxide nanoparticle size on the functional properties of layer-by-layer coated flexible foams, Nanomaterials 11 (2) (2021) 266.
[21] K.M. Holder, M.E. Huff, M.N. Cosio, J.C. Grunlan, Intumescing multilayer thin film deposited on clay-based nanobrick wall to produce self-extinguishing flame retardant polyurethane, J. Mater. Sci. 50 (6) (2015) 2451–2458.
[22] A.F. Thünemann, M. Müller, H. Dautzenberg, J.-F. Joanny, H. Löwen, Polyelectrolyte complexes, editor, in: M. Schmidt (Ed.), Polyelectrolytes With Defined Molecular Architecture II, Springer Berlin Heidelberg, Berlin, Heidelberg, 2004, pp. 113–171.
[23] V.S. Meka, M.K.G. Sing, M.R. Pichika, S.R. Nali, V.R.M. Kolapalli, P. Kesharwani, A comprehensive review on polyelectrolyte complexes, Drug Discov. Today 22 (11) (2017) 1697–1706.
[24] N.A. Vest, A.O. Afonso, D. Rodriguez-Melendez, J. Ponis, D.L. Smith, E.T. Iverson, et al., Polyelectrolyte complex for flame retardant silk, Polym. Degrad. Stab. 216 (2023) 110491.
[25] L. Maddalena, J.M. Indias, P. Bettotti, M. Scarpa, F. Carosio, Cellulose nanocrystals polyelectrolyte complexes as flame retardant treatment for cotton fabrics, Polym. Degrad. Stabil. 220 (2024) 110646.
[26] D. Meng, X. Liu, S. Wang, J. Sun, H. Li, Z. Wang, et al., Self-healing polyelectrolyte complex coating for flame retardant flexible polyurethane foam with enhanced mechanical property, Compos. B: Eng. 219 (2021) 108886.
[27] J. Li, G. van Ewijk, D.J. van Dijken, J. van der Gucht, W.M. de Vos, Single-step application of polyelectrolyte complex films as oxygen barrier coatings, ACS Appl Mater Interfaces 13 (18) (2021) 21844–21853.
[28] A.M. Rumyantsev, N.E. Jackson, Pablo JJd, Polyelectrolyte complex coacervates: recent developments and new frontiers, Annu. Rev. Condens. Matter Phys. 12 (1) (2021) 155–176.
[29] D.L. Smith, M.D. Montemayor, F. Carosio, J.C. Grunlan, Universal intumescent polyelectrolyte complex treatment for cotton, polyester, and blends thereof, Polym. Degrad. Stabil. 228 (2024) 110936.
[30] P. Li, H. Liu, Y.-J. Xu, D.-Y. Wang, Y. Liu, P. Zhu, Flame-retardant and antibacterial flexible polyurethane foams with high resilience based on a P/N/Si-containing system, J. Mater. Sci. Technol. 182 (2024) 141–151.
[31] C.V. Toniciolli Rigueto, M. Rosseto, I. Alessandretti, R. de Oliveira, D.A. R. Wohlmuth, J. Ferreira Menezes, et al., Gelatin films from wastes: a review of production, characterization, and application trends in food preservation and agriculture, Food Res. Int. 162 (2022) 112114.
[32] J.W. Park, W. Scott Whiteside, S.Y Cho, Mechanical and water vapor barrier properties of extruded and heat-pressed gelatin films, LWT - Food Sci. Technol. 41 (4) (2008) 692–700.
[33] MdLLR Menezes, NdR Pires, P.L.R. da Cunha, M. de Freitas Rosa, B.W.S. de Souza, JPdA Feitosa, et al., Effect of tannic acid as crosslinking agent on fish skin gelatin-silver nanocomposite film, Food Packag. Shelf Life 19 (2019) 7–15.
[34] M.C. Gómez-Guillén, B. Giménez, M.E. López-Caballero, M.P. Montero, Functional and bioactive properties of collagen and gelatin from alternative sources: a review, Food Hydrocoll 25 (8) (2011) 1813–1827.
[35] E. Graf, J.W. Eaton, Antioxidant functions of phytic acid, Free Radic. Biol. Med. 8 (1) (1990) 61–69.
[36] B. Stodolak, A. Starzyńska, M. Czyszczoń, K. Żyła, The effect of phytic acid on oxidative stability of raw and cooked meat, Food Chem. 101 (3) (2007) 1041–1045.
[37] Q. Jiang, P. Li, Y. Liu, P. Zhu, Green flame-retardant flexible polyurethane foam based on polyphenol-iron-phytic acid network to improve the fire safety, Compos. B: Eng. 239 (2022) 109958.
[38] W.J. Evans, E.J. McCourtney, R.I. Shrager, Titration studies of phytic acid, J. Am. Oil Chem. Soc. 59 (4) (1982) 189–191.
[39] G. Laufer, C. Kirkland, A.B. Morgan, J.C. Grunlan, Intumescent multilayer nanocoating, made with renewable polyelectrolytes, for flame-retardant cotton, Biomacromolecules 13 (9) (2012) 2843–2848.
[40] P. Li, C. Liu, Q. Jiang, Y. Tao, Y. Xu, Y. Liu, et al., Halogen-free coatings combined with the synergistic effect of phytic acid and montmorillonite for fire safety flexible polyurethane foam, Macromol. Mater. Eng. 307 (5) (2022) 2100930.
[41] L. Yang, H. Liu, N. Hu, Assembly of electroactive layer-by-layer films of myoglobin and small-molecular phytic acid, Electrochem. Commun. 9 (5) (2007) 1057–1061.
[42] L. Maddalena, T. Benselfelt, J. Gomez, M.M. Hamedi, A. Fina, L. Wågberg, et al., Polyelectrolyte-assisted dispersions of reduced graphite oxide nanoplates in water and their gas-barrier application, Acs. Appl. Mater. Inter. 13 (36) (2021) 43301–43313.
[43] J. Dong, Y. Ozaki, K. Nakashima, Infrared, Raman, and near-infrared spectroscopic evidence for the coexistence of various hydrogen-bond forms in poly (acrylic acid), Macromolecules 30 (4) (1997) 1111–1117.
[44] H. Staroszczyk, K. Sztuka, J. Wolska, A. Wojtasz-Pająk, I. Kołodziejska, Interactions of fish gelatin and chitosan in uncrosslinked and crosslinked with EDC films: FT-IR study, Spectrochim. Acta A: Mol. Biomol. Spectrosc. 117 (2014) 707–712.
[45] G. Jiang, J. Qiao, F. Hong, Application of phosphoric acid and phytic acid-doped bacterial cellulose as novel proton-conducting membranes to PEMFC, Int. J. Hydrog. Energy 37 (11) (2012) 9182–9192.
[46] R. Hong, L. Ting, W. Huijie, Optimization of extraction condition for phytic acid from peanut meal by response surface methodology, Resour.-Effic. Technol. 3 (3) (2017) 226–231.
[47] F. Carosio, A. Di Blasio, F. Cuttica, J. Alongi, G. Malucelli, Self-assembled hybrid nanoarchitectures deposited on poly(urethane) foams capable of chemically adapting to extreme heat, RSC Adv. 4 (32) (2014) 16674–16680.
[48] B. Schartel, T.R. Hull, Development of fire-retarded materials—interpretation of cone calorimeter data, Fire Mater. 31 (5) (2007) 327–354.
[49] R.S. Sinha, Clay-Containing Polymer Nanocomposites: from Fundamentals to Real Applications, Newnes, 2013.
[50] C. Hilado, Flammability characteristics of cellular plastics, Ind. Eng. Chem. Prod. Res. Dev. 6 (3) (1967) 154–166.
[51] R.H. Kramer, M. Zammarano, G.T. Linteris, U.W. Gedde, J.W. Gilman, Heat release and structural collapse of flexible polyurethane foam, Polym. Degrad. Stabil. 95 (6) (2010) 1115–1122.
[52] V. Apte, Flammability Testing of Materials Used in Construction, Transport, and Mining, Woodhead Publishing, 2021.
[53] G. Laufer, C. Kirkland, A.A. Cain, J.C. Grunlan, Clay–chitosan nanobrick walls: completely renewable gas barrier and flame-retardant nanocoatings, Acs. Appl. Mater. Inter. 4 (3) (2012) 1643–1649.
[54] A.A. Cain, M.G.B. Plummer, S.E. Murray, L. Bolling, O. Regev, J.C. Grunlan, Iron-containing, high aspect ratio clay as nanoarmor that imparts substantial thermal/flame protection to polyurethane with a single electrostatically-deposited bilayer, J. Mater. Chem. A 2 (41) (2014) 17609–17617.
[55] K.M. Holder, A.A. Cain, M.G. Plummer, B.E. Stevens, P.K. Odenborg, A.B. Morgan, et al., Carbon nanotube multilayer nanocoatings prevent flame spread on flexible polyurethane foam, Macromol. Mater. Eng. 301 (6) (2016) 665–673.

[56] X. Mu, B. Yuan, Y. Pan, X. Feng, L. Duan, R. Zong, et al., A single α-cobalt hydroxide/sodium alginate bilayer layer-by-layer assembly for conferring flame retardancy to flexible polyurethane foams, Mater. Chem. Phys. 191 (2017) 52–61.
[57] H. Pan, Q. Shen, Z. Zhang, B. Yu, Y. Lu, MoS2-filled coating on flexible polyurethane foam via layer-by-layer assembly technique: flame-retardant and smoke suppression properties, J. Mater. Sci. 53 (12) (2018) 9340–9349.
[58] B. Lin, A.C.Y. Yuen, A. Li, Y. Zhang, T.B.Y. Chen, B. Yu, et al., MXene/chitosan nanocoating for flexible polyurethane foam towards remarkable fire hazards reductions, J. Hazard. Mater. 381 (2020) 120952.
[59] F. Carosio, A. Fina, Three organic/inorganic nanolayers on flexible foam allow retaining superior flame retardancy performance upon mechanical compression cycles, Front. Mater. 6 (2019) 20.
[60] R.J. Smith, K.M. Holder, S. Ruiz, W. Hahn, Y. Song, Y.M. Lvov, et al., Environmentally benign halloysite nanotube multilayer assembly significantly reduces polyurethane flammability, Adv. Funct. Mater. (2017).
[61] A. Fahami, J. Lee, S. Lazar, J.C Grunlan, Mica-based multilayer nanocoating as a highly effective flame retardant and smoke suppressant, Acs. Appl. Mater. Inter. 12 (17) (2020) 19938–19943.
[62] D. Ye, C. Wang, J. Xi, W. Li, J. Wang, E. Miao, et al., Construction of sustainable and highly efficient fire-protective nanocoatings based on polydopamine and phosphorylated cellulose for flexible polyurethane foam, Int. J. Biol. Macromol 272 (2024) 132639.
[63] Y. Zeng, Z. Li, Y. Feng, M. Chi, H. Lv, G.-Y Yang, Dual-functional composite coating with flame-retardant and antibacterial properties for flexible polyurethane foams, J. Mater. Chem. A 13 (14) (2025) 9830–9840.
[64] I. Lee, S. Kim, J.O. Shim, J.S. Cho, C. Cho, High flame retardancy of carbon nanotubes reinforced polyelectrolyte multilayered nanocomposites, J. Appl. Polym. Sci. (2025) e56967.
[65] Y. Fang, J. Wu, S. Chang, L. Wu, Flame retardant and anti-dripping polyethylene terephthalate fabric based on bio-based phytic acid/gelatine coating, Surf. Eng. 39 (1) (2023) 49–55.
[66] H. Jiang, Y. Hu, Y. Jiang, K. Yu, R. Qiu, Revealing the flame inhibition effect of phytic acid (PA) by PIV measurements and detailed chemical kinetic modeling of counterflow CH4/PA/air flames, Int. J. Therm. Sci. 208 (2025) 109505.
[67] J. Keränen, J. Hakala, V. Hongisto, The sound insulation of façades at frequencies 5–5000 hz, Build. Env. 156 (2019) 12–20.
[68] X. Li, J.W. Chua, X. Yu, Z. Li, M. Zhao, Z. Wang, et al., 3D-Printed lattice structures for sound absorption: current progress, mechanisms and models, structural-property relationships, and future outlook, Adv. Sci. 11 (4) (2024) 2305232.
[69] J. Lee, I. Jung, Tuning sound absorbing properties of open cell polyurethane foam by impregnating graphene oxide, Appl. Acoust. 151 (2019) 10–21.
[70] P. D'Antonio, Acoustic Absorbers and Diffusers: Theory, Design and Application, CRC Press, 2016.
[71] L. Boeckx, M. Brennan, K. Verniers, J. Vandenbroeck, A numerical scheme for investigating the influence of the three dimensional geometrical features of porous polymeric foam on its sound absorbing behavior, Acta Acust. United Acust. 96 (2) (2010) 239–246.